2016 American Control Conference (ACC)
Boston Marriott Copley Place
July 6-8, 2016. Boston, MA, USA

Frequency response analysis for closed-loop systems with hysteresis using incremental harmonic balance

Lei Fang, Jiandong Wang and Xiaobo Tan

Abstract— **The memory effect of hysteresis seriously hinders the development of effective analysis tools for systems with hysteresis. In this paper a novel incremental harmonic balance method (IHBM) is proposed to compute the steady-state response of a closed-loop system with hysteresis under a sinusoidal excitation, where the play operator is adopted as the hysteresis model. The IHBM method is an iterative algorithm, which assumes that the hysteresis input consists of a series of harmonics, and the small increment in the input harmonics is computed by expanding the hysteresis output as a first-order Taylor approximation and balancing the updated input harmonics to an arbitrary order. One numerical example is provided to demonstrate the advantage of the IHBM over the conventional describing function method in the frequency response analysis of hysteretic systems.**

I. Introduction

The recent several decades have witnessed the rapid development of modeling and control of systems with hysteresis due to the wide application in smart materials [1][2][3][4]. For capturing the hysteresis phenomena in smart materials, an effective model is a cascade system comprising a hysteresis operator and a linear subsystem [5][6]. Among the existing hysteresis operators [7][8], those consisting of a weighted superposition of elementary hysteretic operators are often utilized, for example, the Preisach operator [9][10], the Prandtl-Ishlinskii (PI) operator [11][12], and the Preisach-Krasnosel'skii-Pokrovskii (PKP) operator [13][14]. In control of hysteretic systems, a common technique is to design an inverse operator to compensate the hysteresis effect [6][11].

Compared with the abundant literatures on modeling and control, the studies on analysis of systems with hysteresis are relatively lacked. An critical issue is the memory effect of hysteresis, that is, the output of hysteresis depends not only on the current input as the conventional static nonlinearities do, but also on the whole trajectory of the previous output [8]. The latter characteristic differs hysteresis nonlinearities from the conventional static nonlinearities, and leads to the failure of the existing analysis tools for nonlinear systems with static nonlinearities. Even the basic frequency response analysis for a closed-loop system with hysteresis is challenging. To our knowledge, the existing and effective analysis approach is limited to the describing function method (DFM) [15]. However, as observed latter in Section V, the DFM is only effective when the hysteresis is weak; the performance of the DFM deteriorates rapidly for the system with severe hysteresis, due to the increasing impacts of the high-order harmonic components [16].

In this work, a novel incremental harmonic balance method (IHBM) is proposed to analyze a closed-loop system with hysteresis under a sinusoidal excitation. The IHBM is an iterative algorithm, which assumes that the hysteresis input consists of a series of harmonics, and the small increment in the input harmonics is computed by expanding the hysteresis output as a first-order Taylor approximation and balancing the updated input harmonics to an arbitrary order. The IHBM has been used to analysis of systems with static nonlinearities such as cubic polynomial [17] and dead zone [18]; however, the memory effect of hysteresis makes the direct application of IHBM in hysteretic syst ems challenging. To our best knowledge, this is the first attempt to extend the IHBM to the frequency response analysis for hysteretic systems.

We will deal with the PI operator; however, similar results can be obtained for systems with other hysteresis operators. Since the PI operator consists of a weighted superposition of multiple play operators [11], it suffices to focus on the system with a paly operator. In the application of the IHBM, an issue is how to calculate the harmonics of the periodic output of the play operator under a multi-harmonic input. This problem is addressed by adoption of a novel definition of the play operator, where the play output is described as a complex function dependent of its current input and a series of switching time instants when it enters or exits the boundary region [19]. With the help of bisection method for determining these switching time instants, the input increment is finally formulated as a linear matrix equality and solved efficiently.

The rest of this paper is organized as follows. In Section II the system under consideration is described. The DFM is revisited in Section III. The novel IHBM is illustrated in Section IV. One numerical example is provided in Section V to compare the performance of the IHBM with the DFM. Concluding remarks are given in Section VI.

II. Problem Formulation

Consider a closed-loop system shown in Fig. 1, where the symbol $P[u;m(0)](\cdot)$ is a play operator, and $L_1(s)$ and $L_2(s)$ are two linear components. Generally, $L_1(s)$ can represent

This work was supported in part by the National Natural Science Foundation of China (Nos. 61061130559 and 61174108), China Scholarship Council (No. 201406010203) and by US National Science Foundation (CMMI 1301243).

L. Fang and J. Wang are with College of Engineering, Peking University, Beijing 100871, China. This work was completed during L. Fang's stay at the Smart Microsystems Lab at Michigan State University as a visiting student. {fanglei, jiandong}@pku.edu.cn

X. Tan is with Smart Microsystems Lab, Department of Electrical and Computer Engineering, Michigan State University, East Lansing, MI 48824, USA xbtan@egr.msu.edu

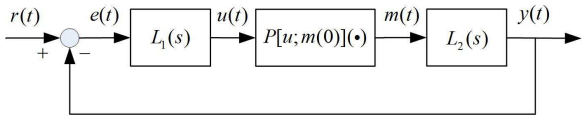

Fig. 1. Configuration of a nonlinear system with a play operator.

a linear controller, while $L_2(s)$ may stand for a controlled linear subsystem. The signals $r(t)$, $e(t)$, $u(t)$, $m(t)$, and $y(t)$ denote the reference, error, play input, play output, and system output, respectively. For a continuous and monotone input $u(t)$ and the initial output $m(0)$, the output $m(t)$ of the play operator $P[u;m(0)](\cdot)$ is calculated by

$$m(t) = P[u;m(0)](t) = \max\{\min\{u(t)+b, m(0)\}, u(t)-b\},$$

where b stands for the play radius. For a non-monotonic input, the output is then calculated by breaking the input into monotone segments and setting the last output of one monotone segment as the initial condition for the next.

Assume that the reference signal $r(t)$ is a sinusoid

$$r(t) = A_r \sin(\omega t), \tag{1}$$

and the steady-state responses of $u(t)$, $m(t)$ and $y(t)$ are periodic with the period $2\pi/\omega$. Assume also that the play input $u(t)$ has an amplitude A_u larger than b, which ensures a contraction property for the play operator and indicates the independence of the play output $m(t)$ on its initial state $m(0)$ [20]. The objective of this paper is to analyze the steady-state responses of $u(t)$, $m(t)$ and $y(t)$ of the closed-loop system in Fig. 1 under the sinusoidal reference $r(t)$ in (1).

III. Describing Function Method

In this paper the conventional DFM is utilized as the benchmark for the frequency response analysis, and compared against the proposed IHBM scheme for the system in Fig. 1. Hence, the DFM is first revisited in this section.

The describing function (DF) of the play operator is easily calculated, and directly given here as [15]

$$|N(A)| = \frac{1}{A}\sqrt{a_1^2+b_1^2}, \tag{2a}$$

$$\underline{/N(A)} = \arctan\left(\frac{a_1}{b_1}\right), \tag{2b}$$

where A is the amplitude of the sinusoidal input of the play operator, and the fundamental harmonic coefficients a_1 and b_1 are

$$a_1 = \frac{4b}{\pi}\left(\frac{b}{A}-1\right),$$
$$b_1 = \frac{A}{\pi}\left[\frac{\pi}{2} - \arcsin(x) - x\sqrt{1-x^2}\right],$$

with $x \triangleq 2b/A-1$.

The effectiveness of the DFM usually requires that the linear components $L_1(s$ and $L_2(s)$ in the closed-loop system be low-pass, because the low-pass property suppresses the higher-order harmonics and then the fundamental harmonic dominates [15]. Under this low-pass assumption, it can be inferred that the signals $e(t)$, $u(t)$ and $y(t)$ are almost sinusoidal of the same frequency under the sinusoidal reference $r(t)$. Then, approximate $u(t)$ as

$$u(t) = A_u \sin(\omega t + \phi_u), \tag{3}$$

and update $m(t)$ by the DF of the play operator in (2) as

$$m(t) = A_u |N(A_u)| \sin\left[\omega t + \phi_u + \underline{/N(A_u)}\right].$$

Because the linear subsystems $L_1(s)$ and $L_2(s)$ have well-defined frequency responses [21], an equation is formulated from $y(t) = r(t) - e(t)$ for the fundamental harmonic component at the angle frequency ω as

$$\begin{aligned} &A_u|N(A_u)||L_2(j\omega)|\sin\left[\omega t + \phi_u + \underline{/N(A_u)} + \underline{/L_2(j\omega)}\right] \\ &= A_r \sin(\omega t) - \frac{A_u}{|L_1(j\omega)|}\sin\left[\omega t + \phi_u - \underline{/L_1(j\omega)}\right], \end{aligned}$$

which gives two equalities in terms of the coefficients of $\sin(\omega t)$ and $\cos(\omega t)$, and uniquely determines the two unknowns A_u and ϕ_u in (3). That is,

$$\begin{aligned} \Phi_1(A_u,\phi_u) \triangleq\ & A_r - \frac{A_u}{|L_1(j\omega)}\cos\left[\phi_u - \underline{/L_1(j\omega)}\right] \\ & - A_u|N(A_u)||L_2(j\omega)|\cos\left[\phi_u + \underline{/N(A_u)} + \underline{/L_2(j\omega)}\right] \\ =\ & 0, \end{aligned} \tag{4a}$$

$$\begin{aligned} \Phi_2(A_u,\phi_u) \triangleq\ & \frac{A_u}{|L_1(j\omega)}\sin\left[\phi_u - \underline{/L_1(j\omega)}\right] \\ & + A_u|N(A_u)||L_2(j\omega)|\sin\left[\phi_u + \underline{/N(A_u)} + \underline{/L_2(j\omega)}\right] \\ =\ & 0. \end{aligned} \tag{4b}$$

It is clear that a numerical method, for example, the Newton-Raphson algorithm [22], is required to solve (4) for A_u and ϕ_u.

IV. Incremental harmonic balance method

This section describes the incremental harmonic balance algorithm for calculating the frequency response of $u(t)$ for the system in Fig. 1.

A. Main idea

Compared with the solution (3) from the DFM, the periodic solution $u(t)$ could be better captured by incorporating higher-order harmonics, i.e.,

$$\begin{aligned} u(t) &= \sum_{n=1}^{N_H} A_{u_n}\sin(n\omega t + \phi_{u_n}) \\ &= \sum_{n=1}^{N_H}\left[a_{u_n}\sin(n\omega t) + b_{u_n}\cos(n\omega t)\right], \end{aligned} \tag{5}$$

where N_H stands for the truncation order of the harmonics, and $a_{u_n} \triangleq A_{u_n}\cos\phi_{u_n}$ and $b_{u_n} \triangleq A_{u_n}\sin\phi_{u_n}$. Note that the DC coefficient of $u(t)$ is zero due to the odd symmetry of the play operator, and is thus not presented in (5). Accordingly, define a sufficiently small increment in $u(t)$ as

$$\begin{aligned} \Delta u(t) &= \sum_{n=1}^{N_H}\Delta A_{u_n}\sin(n\omega t + \Delta\phi_{u_n}) \\ &= \sum_{n=1}^{N_H}\left[\Delta a_{u_n}\sin(n\omega t) + \Delta b_{u_n}\cos(n\omega t)\right], \end{aligned} \tag{6}$$

where $\Delta a_{u_n} \triangleq \Delta A_{u_n}\cos\Delta\phi_{u_n}$ and $\Delta b_{u_n} \triangleq \Delta A_{u_n}\sin\Delta\phi_{u_n}$ with the amplitude conditions $\Delta a_{u_n} \ll a_{u_n}$ and $\Delta b_{u_n} \ll b_{u_n}$.

The main idea of the IHBM is illustrated as follows. The IHBM is an iterative algorithm. At each iteration, the input of the play operator is assumed to consist of a series of harmonics (5), and the corresponding increment (6) in the harmonic input is computed via an incremental harmonic balance technique introduced in the next subsection, then the new input is updated as the summation of the input (5) at the last iteration and the calculated input increment (6); this iteration continues until some convergence criterion is met.

B. Incremental harmonic balance

Expanding the play output $m(t)$ under the updated input $u(t)+\Delta u(t)$ into a first-order Taylor series, one could obtain

$$P[u+\Delta u;m(0)](t) \approx P[u;m(0)](t)+P'[u;m(0)](t)\Delta u(t), \quad (7)$$

where the $'$ denotes the derivative of the play operator with respect to the input u, instead of the conventional time variable t [23]. Then, the symbol $P'[u;m(0)](t)$ is defined as

$$P'[u;m(0)](t) \triangleq \begin{cases} 1, & \text{if } P[u;m(0)](t) \in \prod, \\ 0, & \text{if } P[u;m(0)](t) \in \prod^c. \end{cases} \quad (8)$$

Here, $\prod$ stands for the boundary region of the play operator $P[u;m(0)](t)$, where $m(t) = u(t) \pm b$, and $\prod^c$ is its complement, namely, the interior region, where $m(t)$ is constant. One period of $P[u+\Delta u;m(0)](t)$ and $P[u;m(0)](t)$ can be divided into two subsets dependent of the regions they stay. The first subset is that they both stay in the same region (the boundary or interior region), where the relationship (7) strictly holds. The second case it that one stays in the boundary region and the other stays in the interior region, whose impact is ignorable due to the fact that such time instants have a Lebesgue measure of zero [24] and that $\Delta a_{u_n} \ll a_{u_n}$ and $\Delta b_{u_n} \ll b_{u_n}$. Hence, the approximation in (7) is rational.

In order to continue the harmonic analysis, we have to expand the play output $m(t)$ under the input $u(t)$ into N_H harmonics,

$$\begin{aligned} m(t) &= P[u;m(0)](t) \\ &\approx \sum_{n=1}^{N_H} A_{m_n}\sin(n\omega t+\phi_{m_n}) \\ &= \sum_{n=1}^{N_H} [a_{m_n}\sin(n\omega t)+b_{m_n}\cos(n\omega t)]. \end{aligned} \quad (9)$$

with $a_{m_n} \triangleq A_{m_n}\cos(\phi_{m_n})$ and $b_{m_n} \triangleq B_{m_n}\sin(\phi_{m_n})$. Since the linear components $L_1(s)$ and $L_2(s)$ satisfy the principle of superposition, one equation is reached from $r(t)-e(t)-y(t)=0$, that is,

$$\begin{aligned} \Upsilon(t) \triangleq\ & A_r\sin(\omega t) - \sum_{n=1}^{N_H} \frac{A_{u_n}}{|L_1(jn\omega)|}\sin[n\omega t+\phi_{u_n}-\underline{\angle L_1(jn\omega)}] \\ & - \sum_{n=1}^{N_H} \frac{\Delta A_{u_n}}{|L_1(jn\omega)|}\sin[n\omega t+\Delta\phi_{u_n}-\underline{\angle L_1(jn\omega)}] \\ & - \sum_{n=1}^{N_H} A_{m_n}|L_2(jn\omega)|\sin[n\omega t+\phi_{m_n}+\underline{\angle L_2(jn\omega)}] \\ & - \sum_{n=1}^{N_H} \dot{P}[u;W(0)](t)\Delta A_{u_n}|L_2(jn\omega)|\sin[n\omega t+\Delta\phi_{u_n}+\underline{\angle L_2(jn\omega)}] \\ & \approx 0. \end{aligned} \quad (10)$$

In (10), the second and third terms deal with the harmonics in the input of $L_1(s)$ generating $u(t)$ and $\Delta u(t)$, respectively, while the last two terms result from $P[u+\Delta u;m(0)](t)$ passing $L_2(s)$ with the approximation (7).

The Galerkin's procedure [25] is utilized to balance the coefficients on the terms $\sin(n\omega t)$ and $\cos(n\omega t)$ in (10), which requires $\Upsilon(t)$ be orthogonal to the basis functions $\sin(k\omega t)$ and $\cos(k\omega t)$ in the following sense

$$\begin{aligned} \int_0^{2\pi} \Upsilon(t)\sin(k\omega t)\mathrm{d}(\omega t) &= 0, \\ \int_0^{2\pi} \Upsilon(t)\cos(k\omega t)\mathrm{d}(\omega t) &= 0, \end{aligned}$$

with $k = 1,2,\cdots,N_H$. With the orthogonality of trigonometric functions,

$$\begin{aligned} \int_0^{2\pi} \sin(ix)\sin(jx)\mathrm{d}x &= \begin{cases} 0, & \text{if } i \neq j, \\ \pi, & \text{if } i = j, \end{cases} \\ \int_0^{2\pi} \cos(ix)\cos(jx)\mathrm{d}x &= \begin{cases} 0, & \text{if } i \neq j, \\ \pi, & \text{if } i = j, \end{cases} \\ \int_0^{2\pi} \sin(ix)\cos(jx)\mathrm{d}x &= 0, \quad \forall i,j. \end{aligned}$$

we have (11) (see the top of next page) for $n = 1,2,\ldots,N_H$, where δ_{ij} is a Kronecker delta function, that is, $\delta_{ij} = 1$, if $i = j$; otherwise, $\delta_{ij} = 0$. Equation (11) represents a set of $2N_H$ nonlinear equations, solving uniquely for ΔA_{u_i} and $\Delta\phi_{u_i}$ with $2N_H$ known coefficients A_{u_i} and ϕ_{u_i}, $i = 1,2,\ldots,N_H$.

C. Novel definition of the play operator

Since the harmonic coefficients a_{u_n} and b_{u_n} could be arbitrary, it is difficult to give an analytical harmonic approximation for the play output. As a result, the main challenge in solving (11) is the calculation of A_{m_n} and ϕ_{m_n} in (9) and $P'[u;m(0)](t)$ in (8) for a known multi-frequency sinusoid $u(t)$ in (5). In order to calculate these variables from $u(t)$, we have to access the time instants when the play operator switches between the boundary and the interior regions. For this purpose, the novel definition of the play operator in [19] is utilized. The output $m(t)$ of the play operator is rewritten as

$$m(t) = [u(t)+P_1(t)]P_2(t)+P_3(t),$$

$$\frac{A_{u_n}}{|L_1(jn\omega)|}\cos\left[\phi_{u_n}-\underline{/L_1(jn\omega)}\right]+\frac{\Delta A_{u_n}}{|L_1(jn\omega)|}\cos\left[\Delta\phi_{u_n}-\underline{/L_1(jn\omega)}\right]+A_{m_n}|L_2(jn\omega)|\cos\left[\phi_{m_n}+\underline{/L_2(jn\omega)}\right]$$
$$+\frac{1}{\pi}\int_0^{2\pi}\sum_{k=1}^{N_H}P'[u;m(0)](t)\Delta A_{u_k}|L_2(jk\omega)|\sin\left[k\omega t+\Delta\phi_{u_k}+\underline{/L_2(jk\omega)}\right]\sin(n\omega t)\mathrm{d}(\omega t)=A_r\delta_{1n}, \tag{11a}$$
$$\frac{A_{u_n}}{|L_1(jn\omega)|}\sin\left[\phi_{u_n}-\underline{/L_1(jn\omega)}\right]+\frac{\Delta A_{u_n}}{|L_1(jn\omega)|}\sin\left[\Delta\phi_{u_n}-\underline{/L_1(jn\omega)}\right]+A_{m_n}|L_2(jn\omega)|\sin\left[\phi_{m_n}+\underline{/L_2(jn\omega)}\right]$$
$$+\frac{1}{\pi}\int_0^{2\pi}\sum_{k=1}^{N_H}P'[u;m(0)](t)\Delta A_{u_k}|L_2(jk\omega)|\sin\left[k\omega t+\Delta\phi_{u_k}+\underline{/L_2(jk\omega)}\right]\cos(n\omega t)\mathrm{d}(\omega t)=0. \tag{11b}$$

where the pulse wave signals P_1, P_2 and P_3 are defined as

$$P_1(t)=-b\{\mathrm{sgn}[\dot{u}(t)]\},$$
$$P_2(t)=\begin{cases}0, & t\in[t_{j_0},t_{j_1}),\\ 1, & t\in[t_{j_1},t_{(j+1)_0}),\end{cases}$$
$$P_3(t)=\begin{cases}u(t_{j_0})+r_i\{\mathrm{sgn}[\dot{u}(t_{j_0}^-)]\}, & t\in[t_{j_0},t_{j_1}),\\ 0, & t\in[t_{j_1},t_{(j+1)_0}),\end{cases}$$

with $j=1,2,\cdots$. The symbols t_{j_0} and t_{j_1} are defined as follows. First, assume that the play operator lies in the boundary region before $t=0$. Then, t_{j_0} represents the first time instant after $t_{(j-1)_1}$ when the output $m(t)$ exits from a boundary region and goes into the interior region, that is,

$$\dot{u}(t_{j_0})=0,\ \mathrm{sgn}[\dot{u}(t_{j_0}^-)]\neq\mathrm{sgn}[\dot{u}(t_{j_0}^+)],\ t_{j_0}>t_{(j-1)_1}, \tag{12}$$

and t_{j_1} is the first time instant after t_{j_0} when $m(t)$ moves out of the interior region, which can be further divided into two cases. The first one is that the play operator exits from the boundary region opposite from the one it entered, which is ruled by,

$$|u(t_{j_0})-u(t_{j_1})|\geq 2r_i,\ t_{j_1}\geq t_{j_0}. \tag{13}$$

Another one is that the play operator exits from the same boundary region as the one it entered, namely,

$$\mathrm{sgn}[\dot{u}(t_{j_0}^+)]u(t_{j_1})<\mathrm{sgn}[\dot{u}(t_{j_0}^+)]u(t_{j_0}),\ t_{j_1}\geq t_{j_0}. \tag{14}$$

Note that the calculation of the series of the switching time instants t_{j0} and t_{j1} is strongly based on the details of $u(t)$, and has to be numerical. Here, the series of the time instants t_{j0} and t_{j1} satisfying (12)–(14) are searched for via a bisection method. Note that it is commonly observed that $u(t)$ is sine-like, in that $u(t)$ is odd-symmetric and changes the sign of its derivatives only twice per period [23]. This observation can greatly reduce the computational cost of the proposed IHBM.

D. Formulation of a linear matrix equality

During one period $t\in[0,2\pi/\omega]$, denote $t_0\triangleq 0$ and $t_{M+1}\triangleq 2\pi/\omega$, and define t_i as the time instant when the play operator switches between the interior and boundary regions, $i=1,2,\ldots,M$. Define one new symbol $H(t_i)$ to stand for the value of $P'[u;m(0)](t)$ in (8) over the time interval $[t_i,t_{i+1})$ as

$$H(t_i)=\begin{cases}1, & \text{if } \forall t\in[t_i,t_{i+1}),P[u;m(0)](t)\in\prod,\\ 0, & \text{if } \forall t\in[t_i,t_{i+1}),P[u;m(0)](t)\in\prod^c,\end{cases} \tag{15}$$

where $i=0,1,\ldots,M$. After some necessary deduction from (11), we can derive a linear matrix equation,

$$\begin{bmatrix}C_{11} & C_{12}\\ C_{21} & C_{22}\end{bmatrix}\begin{bmatrix}\Delta a_u\\ \Delta b_u\end{bmatrix}=\begin{bmatrix}R_1\\ R_2\end{bmatrix}. \tag{16}$$

Here, the vectors of the unknowns are $\Delta a_u\triangleq[\Delta a_{u_1},\ \ldots,\ \Delta a_{u_{N_H}}]^T$ and $\Delta b_u\triangleq[\Delta b_{u_1},\ldots,\Delta b_{u_{N_H}}]^T$. The (n,k)-th element of the square coefficient matrix C_{ij}, denoted as $C_{ij}(n,k)$, is

$$\begin{aligned}C_{11}(n,k)=&\ \frac{1}{\pi}\sum_{i=1}^{M}H(t_i)[A_{kn}(i)a_{L_2}(k)+B_{kn}(i)b_{L_2}(k)]\\ &+a_{L_1}^-(n)\delta_{nk}\\ C_{12}(n,k)=&\ \frac{1}{\pi}\sum_{i=1}^{M}H(t_i)[B_{kn}(i)a_{L_2}(k)-A_{kn}(i)b_{L_2}(k)]\\ &+b_{L_1}^-(n)\delta_{nk}\\ C_{21}(n,k)=&\ \frac{1}{\pi}\sum_{i=1}^{M}H(t_i)[B_{nk}(i)a_{L_2}(k)+C_{kn}(i)b_{L_2}(k)]\\ &-b_{L_1}^-(n)\delta_{nk}\\ C_{22}(n,k)=&\ \frac{1}{\pi}\sum_{i=1}^{M}H(t_i)[C_{kn}(i)a_{L_2}(k)-B_{nk}(i)b_{L_2}(k)]\\ &+a_{L_1}^-(n)\delta_{nk}\end{aligned}$$

where $a_{L_2}(n)\triangleq|L_2(jn\omega)|\cos[\underline{/L_2(jn\omega)}]$, $b_{L_2}(n)\triangleq|L_2(jn\omega)|\sin[\underline{/L_2(jn\omega)}]$, $a_{L_1}^-(n)\triangleq\cos[\underline{/L_1(jn\omega)}]/|L_1(jn\omega)|$, and $b_{L_1}^-(n)\triangleq\sin[\underline{/L_1(jn\omega)}]/|L_1(jn\omega)|$, $n=1,\ldots,N_H$. The symbols A_{ij}, B_{ij} and C_{ij} are expressed as

$$\begin{aligned}A_{ij}(k)=&\int_{\omega t_k}^{\omega t_{k+1}}\sin(i\theta)\sin(j\theta)\mathrm{d}\theta\\ B_{ij}(k)=&\int_{\omega t_k}^{\omega t_{k+1}}\cos(i\theta)\sin(j\theta)\mathrm{d}\theta\\ C_{ij}(k)=&\int_{\omega t_k}^{\omega t_{k+1}}\cos(i\theta)\sin(j\theta)\mathrm{d}\theta\end{aligned}$$

The n-th elements in the vectors R_1 and R_2 are

$$\begin{aligned}R_1(n)=&-a_{m_n}a_{L_2}(n)+b_{m_n}b_{L_2}(n)-a_{u_n}a_{L_1}^-(n)\\ &-b_{u_n}b_{L_1}^-(n)+A_r\delta_{1n},\\ R_2(n)=&-b_{m_n}a_{L_2}(n)-a_{m_n}b_{L_2}(n)-b_{u_n}a_{L_1}^-(n)\\ &+a_{u_n}b_{L_1}^-(n).\end{aligned}$$

Finally, the steps of the IHBM are summarized as follows.

1. *Initialization*. Choose N_H. Set the initial value $u^0(t)$ in (5) as the solution (3) from the DFM.
2. *Calculation*. Calculate at the k-th iteration the harmonic approximation of $m^k(t)$ in (9) and the derivative $H^k(t_i)$ in (15), and compute the increment $\Delta u^k(t)$ in (6) from (16).
3. *Update*. Update the harmonic approximation of $u(t)$ with $u^{k+1}(t) = u^k(t) + \Delta u^k(t)$.
4. *Termination*. If the maximum value of $\Delta a_{u_n}^k$ and $\Delta b_{u_n}^k$ $(n = 1, 2, \ldots, N_H)$ is smaller than a given threshold ε_0, then stop; otherwise, set $k = k+1$ and go to Step 2.

Remark that there exists no convergence proof for the IHBM to our knowledge; while extensive numerical simulation indicates that the algorithm converges, it will be of interest to explore rigorous understanding of the convergence properties. Note also that the low-pass property on the linear parts $L_1(s)$ and $L_2(s)$, which is required by the DFM, can be much more relaxed for the IHBM, since the IHBM can use multiple harmonics to better approximate the signals.

V. Numerical Example

One numerical example is provided to validate the performance of the IHBM and compare it against the DFM in frequency response analysis for hysteretic system.

Example 1. In this example, the reference signal is assumed to be $y_r(t) = \sin(\pi t/10)$, and the linear part $L_2(s)$ is $L_2(s) = 1/(8s+1)$. The linear component $L_1(s)$ represents a proportional-integral controller, obtained based on the internal model control rule [26] with closed-loop time constant $\tau_C = 2$ sec, namely, $L_1(s) = 4(1+1/8s)$. The play radius b is a good indicator of the hysteresis severity for the closed-loop system, since as b increases, the hysteresis width increases. The interval for the parameter b is chosen as $[0, 1.2]$. For the IHBM algorithm, we set the two extra parameters as $N_H = 9$ and $\varepsilon_0 = 10^{-8}$.

Define two indices for quantifying the performances of the IHBM and the DFM

$$\mu = \frac{E(|\hat{u} - u|)}{E(|u|)} \times 100\%, \tag{17a}$$

$$Fitness = \left(1 - \frac{\|\hat{u} - u\|}{\|u - E\{u\}\|}\right) \times 100\%. \tag{17b}$$

Here, $\hat{u}$ is the estimation of the play input from the IHBM and the DFM, and u is the one obtained from simulation.

The performance indices in (17) for the IHBM and the DFM are shown in Fig. 2 for $b \in [0, 1.2]$. This figure reveals that the DFM degrades significantly as hysteresis severity b increases, while the IHBM is more robust to the parameter b and much outperforms the DFM. The average iteration number of the IHBM for $N_H = 9$ is 35 in this example, which indicates that the computation cost is minor even we set the tight terminal parameters $\varepsilon_0 = 10^{-8}$.

As a further investigation, the estimates of the play input $\hat{u}(t)$ and play output $\hat{m}(t)$ from the IHBM and the DFM for the case $b = 1.2$ are plotted in Fig. 3. We can see that the estimated play input $\hat{u}(t)$ from the IHBM perfectly

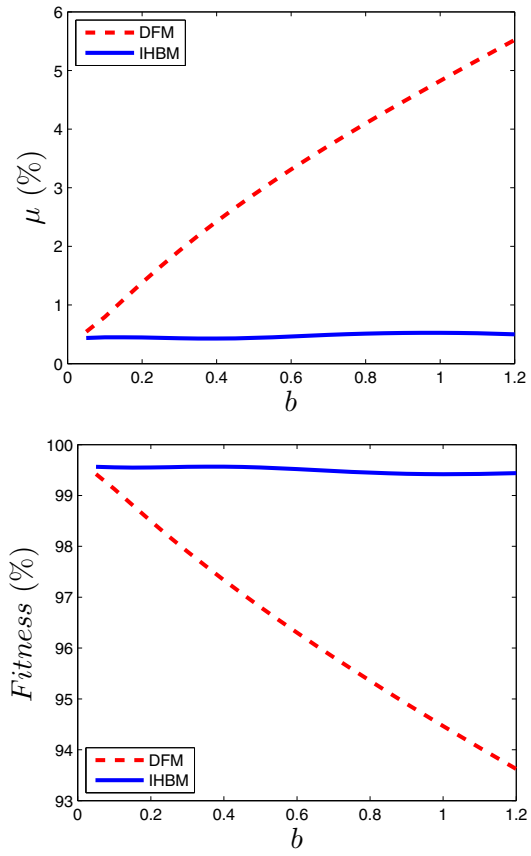

Fig. 2. The performance indices μ (top) and *Fitness* (bottom) calculated from the IHBM and the DFM for $b \in [0, 1.2]$ in Example 1.

overlays with the actual value $u(t)$, while the estimate from the DFM has clear difference from the actual value. The error of the estimate $\hat{m}(t)$ from the DFM is significantly large. Table I quantitatively compares the lower-order harmonic amplitudes A_{u_n} and B_{u_n} of the hysteresis input $u(t)$ from the DFM and the IHBM with the actual values from the spectrum analysis using the fast Fourier transform. The percent error is calculated using the formulation: (Actual-Estimated)/Actual. In Tab. I, the DFM has percentage errors 6.5575% and -0.6407% in estimating the fundamental harmonic components A_{u_1} and B_{u_1}, while the IHBM greatly reduces them to only 0.0780% and 0.0070%. Table I also reveals that the IHBM has good estimation for the third-order harmonic components, which are also not ignorable because $A_{u_3}/A_{u_1} = 1.4533\%$ and $B_{u_3}/B_{u_1} = 6.1630\%$. This example proves that the IHBM is much more accurate than the DFM in dealing with strong hysteresis.

VI. Conclusions and Future Works

In this paper, a novel incremental harmonic balance method was proposed for computing the steady-state response of a closed-loop system with hysteresis under a sinusoidal excitation. The incremental harmonic balance is an iterative algorithm, where the input to hysteresis is assumed to consist of a series of harmonics, and the corresponding

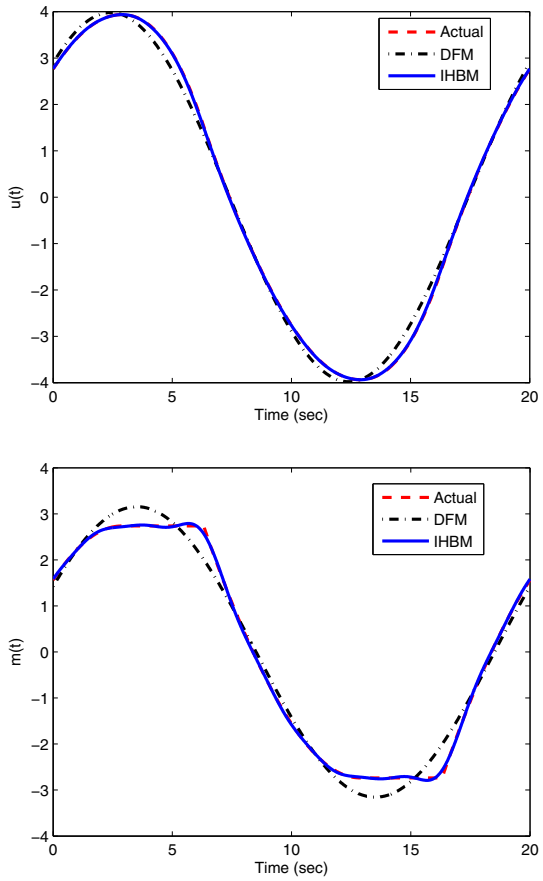

Fig. 3. The comparison of the estimated play input $\hat{u}(t)$ (top) and play output $\hat{m}(t)$ (bottom) from the IHBM and the DFM for $b = 1.2$ in Example 1.

TABLE I

HARMONIC AMPLITUDES A_{u_n} AND B_{u_n} FROM THE IHBM AND THE DFM COMPARED WITH THE ACTUAL VALUES FROM SPECTRUM ANALYSIS FOR EXAMPLE 1.

Coef.	Actual	DFM	Error (%)	IHBM	Error (%)
A_{u_1}	2.8212	2.6362	6.5575	2.8190	0.0780
B_{u_1}	2.8720	2.8904	−0.6407	2.8722	0.0070
A_{u_3}	−0.0410			−0.0414	−0.9756
B_{u_3}	0.1770			0.1761	0.5085

small increment in the input harmonics is computed by expanding the hysteresis output via a first-order Taylor approximation and balancing the updated input harmonics to an arbitrary order. Compared with the traditional describing function method, the proposed approach is able to utilize the harmonics to an arbitrary order; hence, excellent approximation can be achieved even for systems with strong hysteresis, where the describing function method deteriorates considerably due to significant high-order harmonics.

Motivated by the success of the incremental harmonic balance method, we will focus on extending it to analysis of the multi-frequency response of systems with general hysteresis operators consisting of superposition of multiple elementary operators. Another interesting direction is to prove the convergence for the incremental harmonic balance method even under some constraints.

REFERENCES

[1] X. Tan and R. V. Iyer, "Modeling and control of hysteresis: Introduction to the special section," *IEEE Control Syst. Mag.*, vol. 29, no. 1, pp. 26–29, 2009.

[2] M. A. Janaideh, M. Rakotondrabe, and X. Tan, "Guest editorial focused section on hysteresis in smart mechatronic systems: Modeling, identification, and control," *IEEE/ASME Trans. Mechatron.*, vol. 21, no. 1, pp. 1–3, 2016.

[3] R. C. Smith, *Smart Material Systems: Model Development*. Society for Industrial and Applied Mathematics, 2005.

[4] G. Bertotti and I. D. Mayergoyz, Eds., *The Science of Hysteresis Volume I, II and III*. Academic Press, 2005.

[5] J. T. Hsu and K. D. T. Ngo, "A hammerstein-based dynamic model for hysteresis phenomenon," *IEEE Trans. Power Electr.*, vol. 12, no. 3, pp. 406–413, 1997.

[6] R. V. Iyer and X. Tan, "Control of hysteretic systems through inverse compensation," *IEEE Control Syst. Mag.*, vol. 29, no. 1, pp. 83–99, 2009.

[7] M. Brokate and J. Sprekels, *Hysteresis and Phase Transitions*. Springer-Verlag, 1996.

[8] I. D. Mayergoyz, *Mathematical models of hysteresis and their applications*. Academic Press, 2003.

[9] X. Tan and J. S. Baras, "Modeling and control of hysteresis in magnetostrictive actuators," *Automatica*, vol. 40, no. 9, pp. 1469–1480, 2004.

[10] ——, "Adaptive identification and control of hysteresis in smart materials," *IEEE Tran. Autom. Control*, vol. 50, no. 6, pp. 827–839, 2005.

[11] K. Kuhnen, "Modeling, identification and compensation of complex hysteretic nonlinearities: A modified Prandtl-Ishlinskii approach," *Eur. J. Control*, vol. 9, no. 4, pp. 407–418, 2003.

[12] M. A. Janaideh, S. Rakheja, and C. Y. Su, "A generalized Prandtl-cIshlinskii model for characterizing the hysteresis and saturation nonlinearities of smart actuators," *Smart Mater. Struct.*, vol. 18, no. 4, p. p.045001, 2009.

[13] G. V. Webb, D. C. Lagoudas, and A. J. Kurdila, "Hysteresis modeling of SMA actuators for control applications," *J. Intel. Mat. Syst. Str.*, vol. 9, no. 6, pp. 432–448, 1998.

[14] L. Riccardi, D. Naso, H. Janocha, and B. Turchiano, "A precise positioning actuator based on feedback-controlled magnetic shape memory alloys," *Mechatronics*, vol. 22, no. 5, pp. 568–576, 2012.

[15] A. Gelb and W. E. V. Velde, *Multiple-input Describing Functions and Nonlinear System Design*. McGraw-Hill, 1968.

[16] R. E. Mickens, "Comments on the method of harmonic balance," *J. Sound and Vib.*, vol. 94, no. 3, pp. 456–460, 1984.

[17] Y. Chen, J. Liu, and G. Meng, "Incremental harmonic balance method for nonlinear flutter of an airfoil with uncertain-but-bounded parameters," *Appl. Math. Model.*, vol. 36, no. 2, pp. 657–667, 2012.

[18] Y. Shen, S. Yang, and X. Liu, "Nonlinear dynamics of a spur gear pair with time-varying stiffness and backlash based on incremental harmonic balance method," *Int. J. Mech. Sci.*, vol. 48, no. 11, pp. 1256–1263, 2006.

[19] A. Esbrook and X. Tan, "Harmonic analysis for hysteresis operators with application to control design for systems with hysteresis," in *2012 Amer. Control Conf.*, 2012, pp. 1652–1657.

[20] X. Tan and H. K. Khalil, "Two-time-scale averaging of systems involving operators and its application to adaptive control of hysteretic systems," in *2009 Amer. Control Conf.*, 2009, pp. 4476–4481.

[21] A. N. Tripathi, *Linear Systems Analysis*, 2nd ed. New Age Internation Ltd., 1998.

[22] K. E. Atkinson, *An Introduction to Numerical Analysis*. John Wiley & Sons, 2008.

[23] A. Esbrook, X. Tan, and H. K. Khalil, "Self-excited limit cycles in an integral-controlled system with backlash," *IEEE Trans. Autom. Control*, vol. 59, no. 4, pp. 1020–1025, 2014.

[24] V. I. Bogachev, *Measure Theory*. Springer-Verlag, 2007.

[25] C. A. J. Fletcher, *Computational Galerkin Methods*. Springer, 2012.

[26] K. J. Astrom and T. Hagglund, *Advanced PID control*. The Instrumentation, Systems, and Automation Society, 2006.